JOURNAL OF CLINICAL MICROBIOLOGY, Apr. 2004, p. 1614–1619 Vol. 42, No. 4
0095-1137/04/$08.00+0 DOI: 10.1128/JCM.42.4.1614–1619.2004

Simple Algorithm for Identification of *Bordetella pertussis* Pertactin Gene Variants

Gaëtan Muyldermans,[1] Denis Piérard,[1]* Nathalie Hoebrekx,[1] Reza Advani,[2] Shirley Van Amersfoorth,[3] Iris De Schutter,[4] Oriane Soetens,[1] Leo Eeckhout,[1] Anne Malfroot,[4] and Sabine Lauwers[1]

Belgian Reference Laboratory for Pertussis, Department of Microbiology,[1] and Department of Pediatrics,[4] Academisch Ziekenhuis Vrije Universiteit Brussel, Brussels, Belgium; Swedish Institute for Infectious Disease Control, Solna, Sweden[2]; and Research Laboratory for Infectious Diseases, National Institute for Public Health and Environment (RIVM), Bilthoven, The Netherlands[3]

Received 18 July 2003/Returned for modification 5 September 2003/Accepted 12 January 2004

Studies performed in several countries have demonstrated the recent emergence and subsequent dominance of circulating *Bordetella pertussis* strains harboring pertactin and pertussis toxin variants not included in pertussis vaccines. Determination of the pertactin gene variants is commonly performed using a time-consuming and expensive sequence analysis. We developed a simple and reliable pertactin typing algorithm suitable for large-scale screening. The assay correctly identified all pertactin alleles in representative strains. The typing of 231 clinical strains of *B. pertussis* routinely isolated in Belgium showed that this algorithm was adequate to identify less-frequent *prn* types like *prn9* and *prn11*.

Pertussis (whooping cough), mainly caused by *Bordetella pertussis*, is still responsible for high morbidity and mortality among children in many parts of the world. The reemergence of pertussis in several countries with high vaccine coverage (1, 3, 6) has led to renewed interest in whooping cough and in pertussis vaccine efficacy. Vaccine-induced immunity may select among circulating strains for antigenic variants that are divergent from those of the vaccine strains (2, 5, 10, 12, 13). In a recent multilocus sequence typing study based on 15 genes coding for surface proteins, polymorphism was observed in the genes of pertactin (*prn*), pertussis toxin subunits S1 and S3 (*ptxS1* and *ptxS3*), and the tracheal colonizing factor (*tcfA*) (14).

Pertactin, a 69-kDa outer membrane protein, is a major virulence factor of *B. pertussis* that mediates adherence to host cells through an arginine-glycine-aspartic acid (RGD) sequence (8). It is a component of many acellular subunit vaccines. On the basis of polymorphism that occurs mainly in the repetitive region (11), 11 *prn* alleles showing a variable number of GGXXP repeats (Fig. 1A) have been identified (EMBL GenBank database). As demonstrated in isolates collected in The Netherlands and Finland (12, 13), all isolates from the prevaccine period harbored the vaccine pertactin type *prn1*. However, these types were replaced during the 1990s by the nonvaccine *prn* types *prn2* (72 and 27%, respectively, in these two countries), *prn3* (12 and 63%, respectively), and *prn4* (0 and 9%, respectively). For the same period, high prevalences of nonvaccine strains were detected as well in other countries such as Italy (6% *prn1*, 41% *prn2*, 51% *prn3*, and 2% *prn5*), the United States (30% *prn1* and 70% *prn2*), and the United Kingdom (53% non-*prn1*) (2, 5, 10). The allelic variation in *prn* types *prn1* to *prn4*, which represent more than 98% of tested clinical isolates, is restricted to region 1. Typing of these alleles necessitates, therefore, the characterization of this region. However, some less frequent *prn* types (*prn5* to *prn11*) showing variation in other regions have been identified. The determination of the single nucleotide polymorphism T1595G, present in *prn6* to *prn8* and *prn10*, provides a way to further discriminate these rare *prn* types against the predominant *prn* types *prn1* to *prn4*.

After the introduction of the whole-cell vaccine in the 1950s, a progressive shift toward alleles not found in the vaccine strains has been observed. Since the currently circulating isolates differ from the vaccine strains (2, 4, 5, 10, 12, 13, 15), it is important to monitor the corresponding variations, particularly in view of the recent introduction of acellular vaccines in most national immunization programs. The composition of these vaccines is not uniform and differs in the number of antigens, which varies from 1 to 5, and in the antigenic subtypes included. The number of antigens or the inclusion of pertactin (only in vaccines with three or more components) may be responsible for differences in efficacy (7).

Monitoring of clinical isolates by simpler alternatives to sequence analysis improves the turnaround time and expands the analytical capacity to additional strains. So far, the reference method for the determination of the pertactin type has been the sequencing of the *prn* gene (11), a relatively time-consuming and expensive method. Recently, Mäkinen et al. (9) developed a rapid identification method based on real-time PCR in combination with gel electrophoresis. Although the speed and simplicity of this approach make it an advantageous alternative to conventional sequencing of the *prn* gene, this method needs an expensive real-time apparatus and does not differentiate new types such as *prn6* to *prn11*.

We developed a simple method for discriminating the most

* Corresponding author. Mailing address: Department of Microbiology, Academisch Ziekenhuis Vrije Universiteit Brussel, Laarbeeklaan 101, B-1090 Brussels, Belgium. Phone: 32 2 477 50 02. Fax: 32 2 477 50 15. E-mail: denis.pierard@az.vub.ac.be.

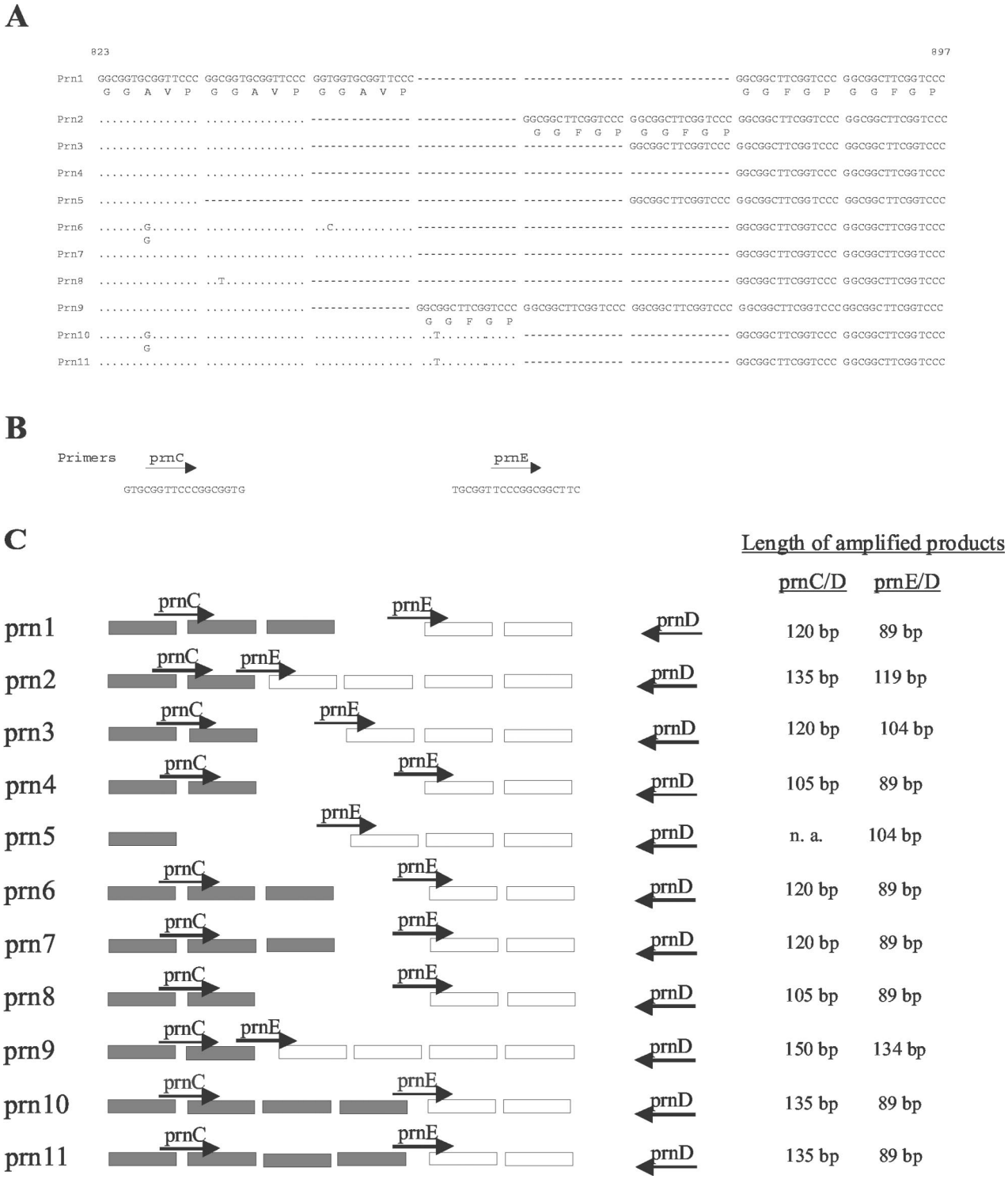

FIG. 1. (A) Polymorphism in the *prn* gene region 1. The 11 known sequences are aligned. Dots represent identical bases; dashes represent deleted bases. The nucleotide numbers correspond to those of *prn1* sequence accession number AJ011091 (GenBank database [http://www.ncbi.nlm.nih.gov/entrez]). (B) Primers prnC and prnE were designed to recognize a region of two constitutive GGAVP repeats and the overlap between GGAVP and GGFGP, respectively. They were used in two separate reactions with the prnD primer that hybridizes with a region downstream of region 1, as shown in panel C. (C) The amplification of isolates with primer pairs prnC-prnD and prnE-prnD allowed us to determine the total number of repeating units (GGAVP and GGFGP) and the number of GGFGP repeating units, respectively (as at right). n. a., no amplification.

TABLE 1. Primers used in this study[a]

Primer	Sequence (5′ to 3′)	Position	Reference
prnC	**G**TGCGGTTCCCGGCGG**TG**	827–844	This study
prnD	GCTCCACGCTGGAGCCCG	946–929	This study
prnE	TGCGGTTCCCGGCGG**CTTC**	858–876	This study
QJF3	GCTGGTGCAGACGCCAG**T**	1605–1622	9
QJF4	GCTGGTGCAGACGCCAG**G**	1605–1622	This study
QJR1	CCGATATCGACCTTGCC	1676–1660	9

[a] The position numbers indicate the position of bases relative to the first start codon of *prn1* (accession number AJ011091). The differences between the primers prnC and prnE as well as those between QJF3 and QJF4 are shown in boldface type.

frequent *prn2* and *prn3* types from the other less frequently occurring variants and to differentiate *prn2* and *prn3* from each other. Further identification of the few remaining isolates can then be performed by either sequencing or real-time PCR. A complete algorithm is proposed and successfully applied to 231 *B. pertussis* isolates, representing almost all the strains isolated in Belgium from 1987 to 2001.

MATERIALS AND METHODS

Strains. The analysis was initially performed on a set of strains representing the different *prn* types kindly provided by J. Mertsola (University of Turku, Turku, Finland) and F. Mooi (National Institute for Public Health and the Environment, Bilthoven, The Netherlands). In addition, 231 clinical *B. pertussis* isolates collected from 1987 through 2001 in our laboratory were used for this study.

Bacteria were grown on Regan-Lowe charcoal agar (Charcoal Agar; Oxoid Ltd., Basingstoke, England) containing 10% horse blood and cephalexin (Bordetella Selective Supplement), incubated during 4 days at 35°C. For PCR, one isolated colony was resuspended in TE (10 mM Tris-HCl [pH 8], 1 mM EDTA) and boiled for 10 min.

Primers. Primers QJF3 and QJR1 were as designed by Mäkinen et al. (9). The others were designed on the basis of sequences available in the GenBank database (http://www.ncbi.nlm.nih.gov/entrez) and are shown in Table 1.

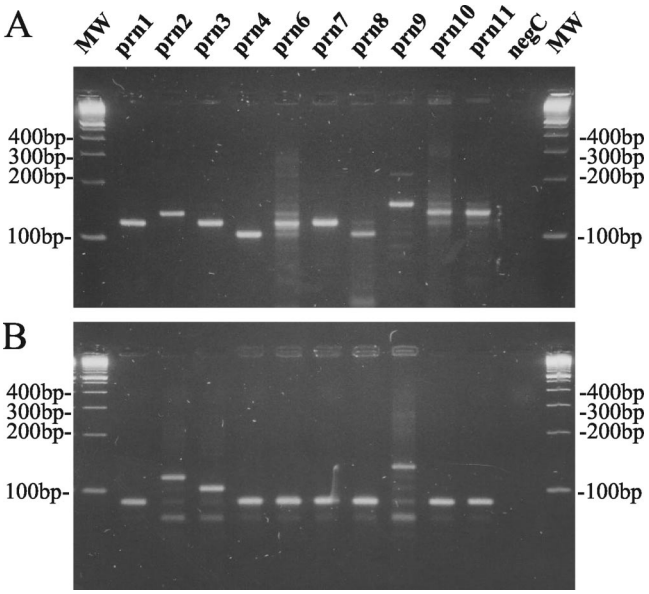

FIG. 2. Ethidium bromide-stained 3% LSI MP agarose (Life Science International) gel containing *B. pertussis* DNA amplified with primer pairs prnC-prnD (A) and prnE-prnD (B) from strains with known *prn* types.

Sequence-specific PCR for typing the repetitive region 1. Two amplifications were performed for the determination of the polymorphism of the *prn* region 1 using either the prnC-prnD or prnE-prnD primer pair (Fig. 1B and C). The PCR method was optimized for the following variables: Mg concentration, annealing temperature, standard or hot-start PCR, number of cycles, and input concentration.

The 50-μl reaction mixture contained 1× Reaction Buffer II (Applied Biosystems, Foster City, Calif.), 1.5 mM $MgCl_2$, a 200 μM concentration of each deoxynucleoside triphosphate, a 1 μM concentration of each primer, and 1 U of Amplitaq Gold DNA polymerase (Applied Biosystems). Amplification was performed in a DNA Thermal Cycler 480 (Applied Biosystems) using the following program: 94°C for 10 min and then 40 cycles of 94°C for 1 min, 66°C for 1 min 30 s, and 72°C for 2 min.

The amplification product was further analyzed on 3% LSI MP agarose (Life Science International, Zellik, Belgium) gel, and the length of the DNA band was compared with those of control samples from *prn1* to *prn4*.

Real-time PCR for the identification of the T1595G point mutation. The real-time PCR method was adapted from that of Mäkinen et al. (8) for SYBR Green I DNA detection. Briefly, two amplifications were performed for the determination of the polymorphism at position 1595. Primer pairs QJF3-QJR1 and QJF4-QJR1 preferentially amplify (i) *prn1* to *prn5*, *prn9*, and *prn11* and (ii) *prn6* to *prn8* and *prn10*, respectively. The PCR mixture was optimized for an I-cycler apparatus (Bio-Rad, Hercules, Calif.) using the qPCR Core Kit for SYBR Green I (Eurogentec, Seraing, Belgium) with the addition of 0.01 μM fluorescein and 1 μl of boiled sample. After an initial denaturation step at 94°C for 10 min, 50 cycles of denaturation at 94°C for 15 s, annealing at 62°C for 15 s, and extension at 72°C for 30 s were performed. Measurement of fluorescence at 495 nm at the end of each extension step allows the detection of the SYBR Green I bound to the amplified double-stranded DNA. The increase in fluorescence signal during the PCR process correlates with PCR product accumulation. The parameter used to type the single nucleotide polymorphism was the cycle threshold (Ct). This is the cycle number at which the reaction begins to be exponential. It is determined by the intersection between the amplification curve and the Ct level, calculated as the 10-fold standard deviation of the observed fluorescence signal between cycles 5 and 20. QJF3 and QJF4 (Table 1) primers were designed to preferentially anneal and extend the alleles with T1595T and T1595G mutations, respectively. Using each of these primers in combination with the antisense QJR1 results in a difference in amplification efficiency. The PCR with the lowest Ct was considered to contain the primers with the most specific binding. After amplification, melting curve analysis of the PCR product was used to differentiate between specific and nonspecific amplification products and thereby confirming the previous amplification result. These curves were obtained by slowly changing the temperature of the reaction solution from 55 to 95°C while continuously collecting fluorescence data. This increase in temperature induces the PCR products to denature, which is accompanied by a decrease in the fluorescence from solutions containing the SYBR Green I dye. To improve the visualization of the melting temperature (T_m), melting peaks were derived from the initial melting curves (relative fluorescence units [RFU] versus temperature [T]) by plotting the negative derivative of fluorescence over temperature versus temperature [$-d(\mathrm{RFU})/dT$ versus T].

Sequencing of the pertactin gene. Sequencing of the *prn* gene from isolates Bord4, Bord49, and Bord68 was performed as described by Mooi et al. (13).

RESULTS

Development of the sequence-specific PCR for the identification of *prn* region 1 polymorphism. The polymorphism in the *prn* gene is mainly confined to region 1 (13). The number of repetitive GGXXP units in region 1 was determined by two sequence-specific PCR tests as shown in Fig. 1. These reactions were performed on a representative isolate from each *prn* type as described in Materials and Methods, except for *prn5*, for which no isolate was available. Using the primer pair prnC-prnD, amplification fragments were obtained with different lengths corresponding to the total number of repeat units GGAVP and GGFGP (Fig. 1C). This allowed us to discriminate the *prn1*, *prn3*, *prn6*, and *prn7* types (120-bp fragment) from the *prn2*, *prn10*, and *prn11* types (135-bp fragment), the *prn4* and *prn8* types (105-bp fragment), and the *prn9* type

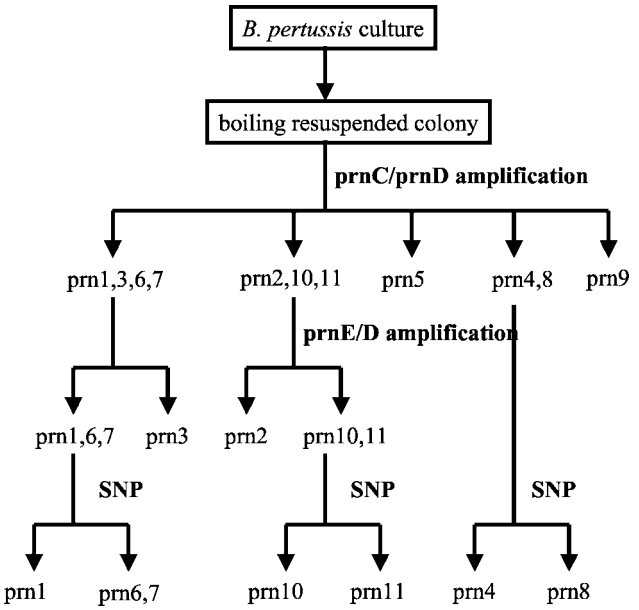

FIG. 3. Workflow for typing *prn* alleles. The sequence-specific PCR method using the primer pairs prnC-prnD and prnE-prnD allows the efficient identification of the major types *prn2* and *prn3*. A further identification of the minor types *prn1* and *prn4* to *prn11* can then be performed by a single nucleotide polymorphism determination method (SNP) by either real-time PCR or sequencing.

(150-bp fragment) as shown in Fig. 2A. Due to the presence of point mutations in the prnC primer binding site (Fig. 1A and B), it was not possible to obtain single DNA bands for some *prn* types. Lowering the specificity of PCR conditions (increasing the Mg concentration or decreasing the annealing temperature) increased the number and intensity of the secondary bands on agarose gel, while increasing the specificity of PCR conditions resulted in the disappearance of the appropriate fragments for *prn6*, *prn8*, and *prn10* (data not shown).

On the other hand, with the primer pair prnE-prnD, amplification fragments with different sizes corresponding to the number of GGFGP repeat units (Fig. 1C) were obtained. It allowed us to discriminate the *prn* types *prn1*, *prn4*, *prn6*, *prn7*, *prn8*, *prn10*, and *prn11* (89-bp fragment) from types *prn3* (104-bp fragment), *prn2* (119-bp fragment), and *prn9* (134-bp fragment) as shown in Fig. 2B.

Compared to previous sequencing data (Fig. 1A), all type strains were correctly categorized by this PCR method. Combining the two sequence-specific amplification methods allowed us to differentiate the most frequent *prn* types, *prn2* and *prn3*, from the others as summarized in Fig. 3. In addition, this method allowed us to discriminate the 11 known *prn* types into the following seven groups: *prn1*, *prn6*, and *prn7*; *prn2*; *prn3*; *prn4* and *prn8*; *prn5*; *prn9*; and *prn10* and *prn11*.

Real-time PCR for the identification of the T1595G point mutation. As the determination of polymorphism with the sequence-specific PCR developed in-house was unable to discriminate the *prn1* type from the rare *prn6* or *prn7* type, we performed a SYBR Green I real-time PCR adapted from a previously described method (9). This method could discriminate *prn4* from *prn8* and *prn10* from *prn11* as well.

Primers QJF3 and QJF4 differ by only one nucleotide at the 3′ end (Table 1). Since the *prn* types *prn1* to *prn5*, *prn9*, and *prn11* contain a T at position 1595, these type strains are preferentially recognized by the QJF3 primer, which contains a T at the 3′ end. Preferential amplification is obtained with this sense primer in combination with the antisense QJR1 primer compared to the QJF4-QJR1 pair. On the other hand, as *prn6* to *prn8* and *prn10* contain a G at position 1595, these alleles are preferentially amplified by the QJF4-QJR1 primer pair. In Fig. 4A a comparison of the amplification profiles from *prn1* and *prn7* are shown for the real-time amplification with the primer pairs QJF3-QJR1 and QJF4-QJR1. The lower value of the intersection between the curve and the Ct level with primer pair QJF3-QJR1 (30.7) compared to that for primer pair QJF4-QJR1 (37.4) confirms that T1595T is present in the *prn1* allele. In contrast, the Ct for the *prn7* using the primer pair QJF4-QJR1 is 15 cycles lower than that obtained with QJF3-QJR1. The melting curve analysis confirmed this interpretation, as a specific melting peak was observed for the *prn1* strain amplified with the QJF3-QJR1 primer pair at 88.0°C and not for the QJF4-QJR1 primer pair (Fig. 4B). For the *prn7* strain, a specific melting peak (88.5°C) was observed only with the QJF4-QJR1 amplification. No specific amplification could be detected for the negative control and the melting curve analysis did not show any peak (data not shown).

Table 2 summarizes the Ct for the representative strains and their T_ms. The mean T_m was 88.0°C (range, 87.5 to 88.5°C).

Use of the *prn* typing algorithm for typing clinical isolates. A total of 231 clinical isolates collected in Belgium from 1987 through 2001 were typed using our algorithm (Fig. 3): 22 (9.5%), 140 (60.6%), and 66 (28.6%) contained *prn1*, *prn2*, and *prn3*, respectively. The sequence-specific PCR allowed us to discriminate three isolates (Bord4, Bord49, and Bord68) with *prn* types differing from the more-frequent *prn* types *prn1* to *prn3*. Since Bord4 and Bord68 contained a 149-bp fragment in the amplification reaction mixture with primer pair prnC-prnD (Fig. 5A), *prn* genes from both isolates were classified as *prn9*. The presence of the 134-bp fragment in the amplification reaction mixture using the primer pair prnE-prnD (Fig. 5B) and the presence of the T1595T mutation confirmed this result (Table 2). On basis of the presence of the 134- and 89-bp fragments for the amplification reaction mixture using primer pairs prnC-prnD and prnE-prnD, respectively (Fig. 5), the *prn* gene from isolate Bord49 was classified as a *prn10* or *prn11*. The presence of the T1595T mutation as shown by the real-time PCR (Table 2) allowed us to further characterize this gene as a *prn11*. The type of these three rare *prn* variants was subsequently confirmed by sequence analysis (GenBank accession numbers AY382174, AY382175, and AY382176).

DISCUSSION

Sequencing the *prn* gene in regions 1 and 2 is probably the most accurate method for typing the *prn* gene. It was previously demonstrated in numerous studies that *prn1*, *prn2*, and *prn3* types predominate in different parts of the world (2, 4, 5, 10, 12, 13, 15). Since these types differ only in region 1, it was proposed that region 1 in all isolates should be sequenced and when a novel variant of region 1 was found, that the complete *prn* gene should be sequenced (11). However, this method is time-consuming and expensive.

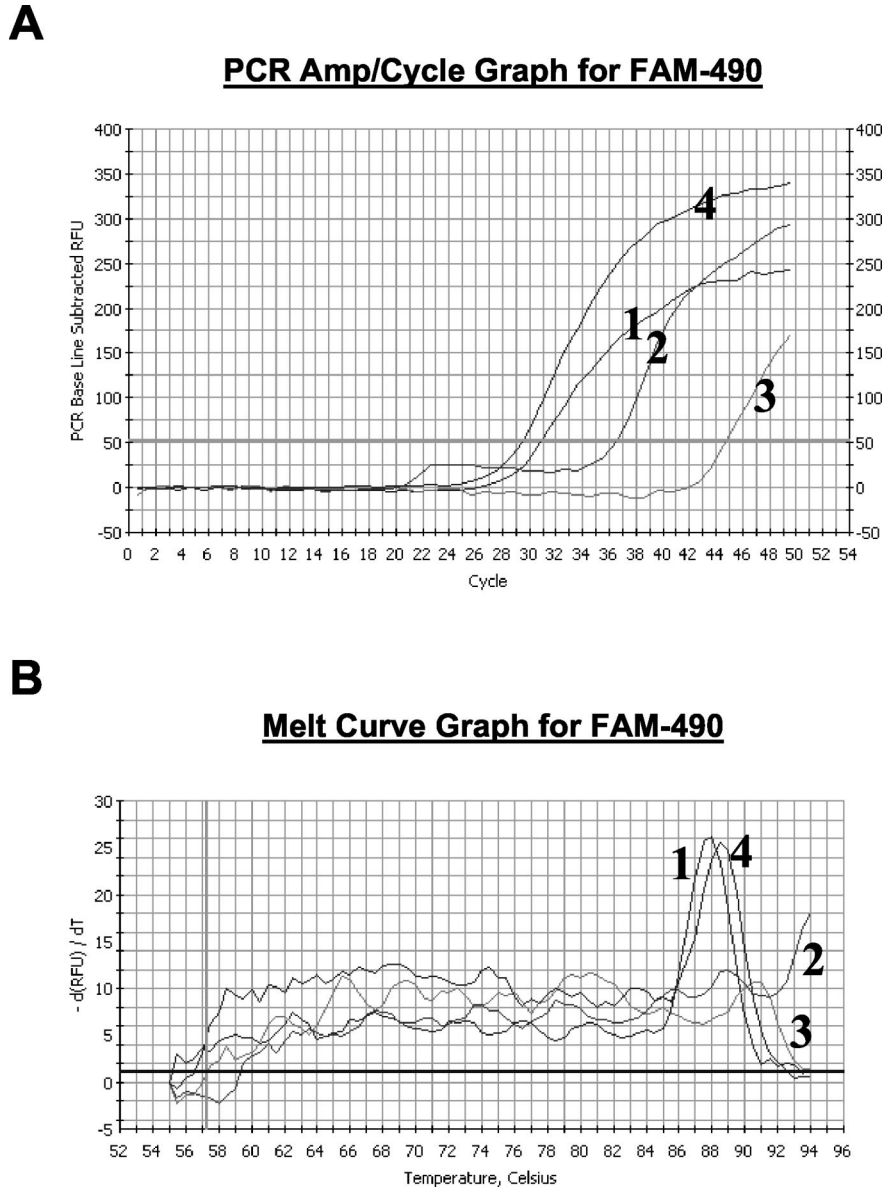

FIG. 4. (A) Amplification profiles of real-time PCR with SYBR Green I. Curves 1 and 2, amplification profile for a representative *prn1* strain with primer pairs QJF3-QJR1 and QJF4-QJR1, respectively; curves 3 and 4, amplification profile for a representative *prn7* strain with primer pairs QJF3-QJR1 and QJF4-QJR1, respectively. (B) Melting curves from the specific amplification assays shown in panel A.

In this study, a simple algorithm was developed for typing the *prn* gene from *B. pertussis*. The method proved to be accurate and has a short turnaround time of 1 day. It allows the differentiation of the common *prn* types *prn1* to *prn3* from each other. Although *prn6* and *prn7* could not be differentiated, the method allows the identification of less-frequent *prn* types. Furthermore, it is convenient for large-scale screening while rapidly providing an epidemiologic overview of the circulating strains. With these advantages, this method is a convenient alternative to the expensive and time-consuming sequence typing method. An important characteristic of the algorithm is the possibility to detect novel types as shown by the characterization of the three isolates with rare *prn* types.

The algorithm used in this work is based on two amplification reactions using the primer pairs prnC-prnD and prnE-prnD. The former was mainly used for the differentiation of known *prn* types, with the latter providing additional discrimination and/or confirmation. Due to the presence of point mutations in the prnC primer binding site (Fig. 1A and B), it was not possible to fully optimize the PCR test. The presence of aspecific bands for some rare isolates demonstrates that the PCR conditions are highly critical. Whenever these aspecific bands are observed, performing the described real-time PCR or sequencing of the *prn* gene is necessary to confirm the observed types.

The primer pairs prnC-prnD and prnE-prnD were specifically designed for the differentiation of *prn1* to *prn4*, the only types that were known at the initiation of the study. Using both

TABLE 2. Ct values for representative *prn* strains and clinical isolates with rare *prn* types for the QJF3-QJR1 and QJF4-QJR1 amplifications

Strain	*prn* type	Ct value (T_m[a] [°C]) for:		Result
		QJF3-QJR1	QJF4-QJR1	
	prn1	30.7 (88.0)	37.4 (—)	1595T
	prn2	29.5 (88.0)	36.5 (—)	1595T
	prn3	29.6 (80.0)	36.6 (—)	1595T
	prn4	28.2 (87.5)	38.9 (—)	1595T
	prn6	41.7 (—)	28.9 (88.5)	1595G
	prn7	44.5 (—)	29.7 (88.5)	1595G
	prn8	40.8 (—)	27.3 (88.5)	1595G
	prn9	28.8 (88.0)	35.9 (—)	1595T
	prn10	40.0 (—)	27.9 (88.5)	1595G
	prn11	29.1 (88.0)	35.1 (—)	1595T
Bord4	*prn9*	34.1 (87.5)	40.2 (—)	1595T
Bord49	*prn11*	32.4 (88.5)	42.7 (—)	1595T
Bord68	*prn9*	25.8 (87.5)	36.2 (—)	1595T
Negative control		>50 (—)	45.7 (—)	Negative

[a] T_m of the main peak. —, no specific melting peak observed.

amplifications, we succeeded in differentiating the 11 types known at present into seven groups. These groups were further differentiated by an additional real-time PCR method. Since the difference in the number of repeat units results in a size difference of only 15 bp, we designed a PCR in which short amplification products were obtained, allowing us to differentiate the types on basis of the differences in amplification fragments. In order to accurately estimate the size of the obtained fragments, a high-resolution agarose gel was needed, and the amplification products were always compared to those of the positive controls.

Our study demonstrated that 98% of the Belgian isolates belong to the *prn* types *prn1* to *prn3*. As much as 9% still belong to the *prn1* type, the *prn* type of the strains that are included in the conventional whole-cell vaccine. Since no isolates are available for the prevaccination period in Belgium, no comparison could be performed for this period.

This method is convenient for large-scale screening of all available isolates in a short time rather than typing a fraction of the collected isolates when sequencing is performed. In the future, application of this method—which is faster and less laborious than sequencing—to other genetic loci such as *ptxS1*, *ptxS3*, and *tcfA* will improve the monitoring of the strains. Finally, this method will also be a useful tool for the collection of typing data from the pre- and post-acellular vaccine eras.

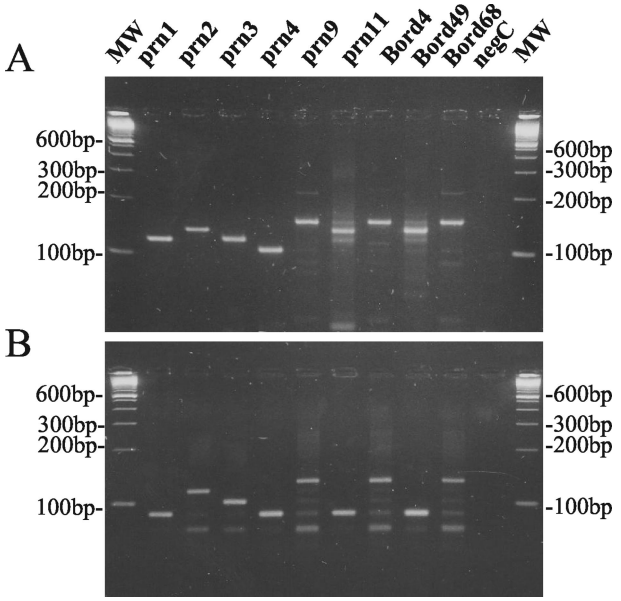

FIG. 5. Ethidium bromide-stained 3% LSI MP agarose (Life Science International) gel containing *B. pertussis* DNA amplified with primer pairs prnC-prnD (A) and prnE-prnD (B).

ACKNOWLEDGMENT

This work was supported by OZR grant 624 (Vrije Universiteit Brussel, Brussels, Belgium).

REFERENCES

1. **Andrews, R., A. Herceg, and C. Roberts.** 1997. Pertussis notifications in Australia, 1991 to 1997. Commun. Dis. Intell. **21:**145–148.
2. **Cassiday, P., G. Sanden, K. Heuvelman, F. Mooi, K. M. Bisgard, and T. Popovic.** 2000. Polymorphism in *Bordetella pertussis* pertactin and pertussis toxin virulence factors in the United States, 1935–1999. J. Infect. Dis. **182:** 1402–1408.
3. **De Melker, H. E., J. F. Schellekens, S. E. Neppelenbroek, F. R. Mooi, H. C. Rumke, and M. A. Conyn-Van Spaendonck.** 2000. Reemergence of pertussis in the highly vaccinated population of the Netherlands: observations on surveillance data. Emerg. Infect. Dis. **6:**348–357.
4. **De Schutter, I., A. Malfroot, I. Dab, N. Hoebrekx, G. Muyldermans, D. Piérard, and S. Lauwers.** 2003. Molecular typing of *Bordetella pertussis* isolates recovered from Belgian children and their household members. Clin. Infect. Dis. **36:**1391–1396.
5. **Fry, N. K., S. Neal, T. G. Harrison, E. Miller, R. Matthews, and R. C. George.** 2001. Genotypic variation in the *Bordetella pertussis* virulence factors pertactin and pertussis toxin in historical and recent clinical isolates in the United Kingdom. Infect. Immun. **69:**5520–5528.
6. **Guris, D., P. M. Strebel, B. Bardenheier, M. Brennan, R. Tachdjian, E. Finch, M. Wharton, and J. R. Livengood.** 1999. Changing epidemiology of pertussis in the United States: increasing reported incidence among adolescents and adults, 1990–1996. Clin. Infect. Dis. **28:**1230–1237.
7. **Jefferson, T., M. Rudin, and C. Di Pietrantonj.** 2003. Systematic review of the effects of pertussis vaccines in children. Vaccine **21:**2012–2023.
8. **Leininger, E., C. A. Ewanowich, A. Bhargava, M. S. Peppler, J. G. Kenimer, and M. J. Brennan.** 1992. Comparative roles of the Arg-Gly-Asp sequence present in the *Bordetella pertussis* adhesins pertactin and filamentous hemagglutinin. Infect. Immun. **60:**2380–2385.
9. **Mäkinen, J., M. K. Viljanen, J. Mertsola, H. Arvilommi, and Q. He.** 2001. Rapid identification of *Bordetella pertussis* pertactin gene variants using LightCycler real-time polymerase chain reaction combined with melting curve analysis and gel electrophoresis. Emerg. Infect. Dis. **7:**952–958.
10. **Mastrantonio, P., P. Spigaglia, H. van Oirschot, H. G. van der Heide, K. Heuvelman, P. Stefanelli, and F. R. Mooi.** 1999. Antigenic variants in *Bordetella pertussis* strains isolated from vaccinated and unvaccinated children. Microbiology **145:**2069–2075.
11. **Mooi, F. R., H. Hallander, C. H. Wirsing von Konig, B. Hoet, and N. Guiso.** 2000. Epidemiological typing of *Bordetella pertussis* isolates: recommendations for a standard methodology. Eur. J. Clin. Microbiol. Infect. Dis. **19:** 174–181.
12. **Mooi, F. R., Q. He, H. van Oirschot, and J. Mertsola.** 1999. Variation in the *Bordetella pertussis* virulence factors pertussis toxin and pertactin in vaccine strains and clinical isolates in Finland. Infect. Immun. **67:**3133–3134.
13. **Mooi, F. R., H. van Oirschot, K. Heuvelman, H. G. van der Heide, W. Gaastra, and R. J. Willems.** 1998. Polymorphism in the *Bordetella pertussis* virulence factors P.69/pertactin and pertussis toxin in The Netherlands: temporal trends and evidence for vaccine-driven evolution. Infect. Immun. **66:** 670–675.
14. **van Loo, I. H., K. J. Heuvelman, A. J. King, and F. R. Mooi.** 2002. Multilocus sequence typing of *Bordetella pertussis* based on surface protein genes. J. Clin. Microbiol. **40:**1994–2001.
15. **Weber, C., C. Boursaux-Eude, G. Coralie, V. Caro, and N. Guiso.** 2001. Polymorphism of *Bordetella pertussis* isolates circulating for the last 10 years in France, where a single effective whole-cell vaccine has been used for more than 30 years. J. Clin. Microbiol. **39:**4396–4403.